Ab Initio Study of the Mechanism of the Binding of Triplet O_2 to Hemocyanin

Fernando Bernardi,[†] Andrea Bottoni,*[,†] Rita Casadio,[‡] Piero Fariselli,[§] and Adelio Rigo[§]

Dipartimento di Chimica "G. Ciamician", Università di Bologna, Via Selmi 2, Bologna, Italy, Laboratorio di Biofisica, Dipartimento di Biologia, Università di Bologna, Via Irnerio 42, Bologna, Italy, and Dipartimento di Chimica Biologica, Università di Padova, Via Trieste 75, Padova, Italy

Received January 31, 1996[⊗]

Accurate DFT computations have been carried out to investigate the mechanism of oxygen binding to hemocyanins using two different model systems. The simpler model (model 1) is formed only by a Cu^+-Cu^+ dimer and by the approaching oxygen molecule, while the more complex model (model 2) involves also four ammonia molecules (bonded to the metal atoms) which emulate the real histidine ligands of the protein matrix. The computational results point out the inadequacy of model 1 in describing the oxygen binding process and show that the greater stability of the singlet versus the triplet state of the final complex (experimentally observed) is not an intrinsic property of the oxygenated copper dimer but is due to the presence of the copper ligands which are responsible for the occurrence of an intersystem crossing along the reaction coordinate. The ligand effect has been rationalized using a simple MO model which considers the interactions occurring between the nitrogen lone pairs of the ligands and the orbitals that describe the bonding in the $Cu^+(O-O)Cu^+$ fragment.

Introduction

Hemocyanins are well-known oxygen carrier proteins found in mollusks and arthropods. They are characterized by a binuclear copper active site that binds oxygen as peroxide, producing oxyhemocyanins. These proteins have been extensively studied. The three-dimensional structure of the deoxygenated form of hemocyanins from *Panulirus interruptus* was first determined by Volbeda and Hol.[1] From these data it is evident that the active site, formed by two copper ions in the Cu(I) oxidation state, is embedded in the protein matrix with three histidine residues coordinating each copper ion.

Very recently high-resolution X-ray crystal structures of hemocyanins and oxyhemocyanins from *Limulus poliphemus* have become available.[2] These data indicate that each copper is tightly coordinated in a square-planar geometry to both atoms of the oxygen molecule and to the nitrogen atoms of the two closer histidine ligands. The third histidine ligand is placed axially and coordinates each copper atom more weakly. The two copper, the two oxygen, and the four nitrogen atoms lie approximately in the same plane with the molecular oxygen in a side-on (μ-η^2:η^2) configuration with respect to the Cu−Cu axis. The distance between the two coppers is 3.54 Å, while the oxygen atoms are 1.41 Å apart (see Figure 1). While in this structure the relative positions of the copper atoms and histidine molecules are very similar to those found by Volbeda and Hol,[1] the data obtained for the deoxygenated form of the protein from *L. poliphemus* are somewhat different. In this case the two coppers of the active site are each trigonally coordinated by three histidines with a Cu−Cu distance of 4.6 Å (see Figure 2), which is appreciably greater than the value found in the deoxygenated *Panulirus* hemocyanin (3.5 Å).[1] The difference found between the deoxygenated *Panulirus* structure and the deoxygenated *Limulus* structure has been explained with a two-state model, where the hemocyanin hexamer adopts conformational states of high (R-state) or low (T-state) oxygen affinity that may be oxygenated or deoxygenated. It has been postulated that, while the deoxygenated form of *Limulus* hemocyanin is in the T-state, the *Panulirus* structure described by Volbeda and Hol resembles a deoxygenated R-state.[2a]

In addition to structural data, many other experimental results, obtained using different spectroscopic methods (Raman,[3] UV,[4] EPR,[3b,c,4] and EXAFS[5]), are available for the oxygenated and

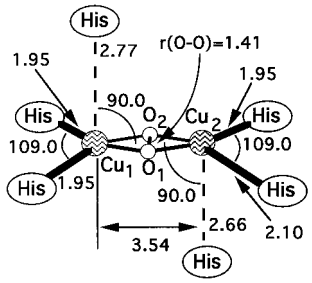

Figure 1. Experimental geometry of the oxygenated hemocyanin from *Limulus poliphemus*. The His symbols indicate the histidine ligands of the protein matrix (bond lengths are in angstroms and angles in degrees).

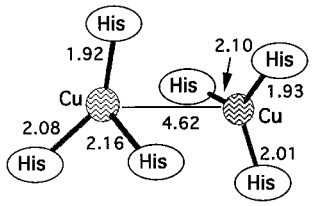

Figure 2. Experimental geometry of the hemocyanin from *Limulus poliphemus*. The His symbols indicate the histidine ligands of the protein matrix (bond lengths are in angstroms and angles in degrees).

[†] Dipartimento di Chimica "G. Ciamician", Università di Bologna.
[‡] Dipartimento di Biologia, Università di Bologna.
[§] Università di Padova.
[⊗] Abstract published in *Advance ACS Abstracts*, July 15, 1996.

(1) Volbeda, A.; Hol, W. G. J. *J. Mol. Biol.* **1989**, *209*, 249.
(2) Magnus, K.; Ton-That, H.; Carpenter, J. E. In *Bioinorganic Chemistry of Copper*; Karlin, K. D., Tyeklar, Z., Eds.; Chapman & Hall: New York, 1993; pp 143−150. Magnus, K.; Hazes, B.; Ton-That, H.; Bonaventura, C.; Bonaventura, J.; Hol, W. G. J. *Protein Struc. Func. Gen.* **1994**, *19*, 302.
(3) (a) Loehr, J. S.; Freedman, T. B.; Loehr, T. M. *Biochem. Biophys. Res. Commun.* **1974**, *56*, 510. (b) Freedman, T. B.; Loehr, J. S.; Loehr, T. M. *J. Am. Chem. Soc.* **1976**, *98*, 2809. (c) Larrabee, J. A.; Spiro, T. G. *J. Am. Chem. Soc.* **1980**, *102*, 4217.

S0020-1669(96)00102-4 CCC: $12.00

deoxygenated form of hemocyanins. EXAFS data,[5] for example, show the existence of a vacancy in the copper ion d shell of oxyhemocyanin. They also show that the two copper atoms in oxyhemocyanin are both in the cupric Cu(II) oxidation state, indicating that, upon oxygen binding, an electron transfer takes place from the two Cu(I) cations to the dioxygen. Accordingly, the resonance Raman spectrum reveals a very low energy O−O stretching vibration (750 cm^{-1}) as compared to an isolated oxygen molecule (1550 cm^{-1}). This result suggests that, upon oxygen binding, there is an increase of the O−O bond length due to electron transfer from the cations to the O_2 ligand. Another relevant experimental result which has given useful suggestions on the electronic structure of the oxygenated active site is the absence of any EPR signal in oxyhemocyanins. Magnetic susceptibility studies show that this behavior, which excludes the presence of unpaired electrons, is due to a strong antiferromagnetic coupling between the two Cu(II) ions to form singlet and triplet states, with the triplet higher in energy than the singlet by a value greater than 600 cm^{-1}. This large antiferromagnetic coupling requires orbital overlap between the two Cu(II) cations. Since the distance between these cations is about 3.5 Å, they must be coupled through a superexchange mechanism which implies the presence of a bridging ligand between the two metal ions. The structural data have demonstrated that the only bridging ligand responsible for the superexchange pathway is the oxygen molecule.[2]

Only a limited number of theoretical investigations have been performed so far for modeling the copper−peroxide complex.[6] These studies, which have been accomplished for the most part before X-ray crystallographic information was available, have provided information which are in agreement with the experiment. Solomon carried out SCF-Xα-scattered wave (SCF-Xα-SW) calculations on a model compound formed by the $(Cu^+)_2-O_2$ complex with four in-plane NH_3 ligands to emulate the histidine ligands.[6a−c] Maddaluno performed *ab initio* ROHF-GVB computations on various geometrical arrangements of the $Cu^+(O-O)Cu^+$ complex without introducing any additional ligand to simulate the histidine molecules.[6d] Both SCF-Xα and *ab initio* ROHF-GVB computations indicated the side-on (μ-η^2:η^2) configuration as the most likely geometry, with the singlet state more stable than the triplet state, and the O_2 molecule as the bridging ligand responsible for the superexchange mechanism between the two copper ions.

Very recently[6f] we have carried out an *ab initio* study on the active site of oxyhemocyanin using both a density functional theory approach (DFT) and a CASSCF approach followed by a perturbation treatment up to second order (CASPT2)[7] to evaluate the dynamic correlation contribution. The purpose of this work was to investigate the nature of the singlet and triplet wave functions, using accurate ab initio methods with various basis sets, and the effects of ligands on the oxyhemocyanin complex. We have demonstrated that the greater stability of the singlet versus the triplet state (experimentally observed) is not an intrinsic property of the oxygenated copper binuclear site but depends on the presence of the ligands on the copper atoms. However, to our knowledge no *ab initio* studies have yet been devoted to investigate in detail the binding process of triplet oxygen to the active site of hemocyanin to form the singlet oxyhemocyanin complex. In the present paper we investigate in detail the mechanism of this process, focusing on two different models of the oxygen binding site (see Figure 3). The first model (model 1) consists of an oxygen molecule which approaches a copper dimer, where no ligands have been considered. The second model (model 2) is characterized by the presence of four NH_3 molecules which emulate the in-plane histidine ligands. We have demonstrated in our previous work[6f] that the presence of two additional NH_3 molecules (which should simulate the two additional histidine ligands that are placed axially) does not significantly change the results (the variation of the singlet−triplet energy gap is in fact very small) and that the ammonia molecules satisfactorily represent the real histidine ligands. For both models 1 and 2 we compute the singlet and triplet energy profiles associated with the approaching of the oxygen molecule to the binuclear protein active site. To this purpose we use a DFT approach, since we have demonstrated that this method provides the correct energy order for the electronic states of the final complex. Furthermore, we assume for model 2 that the deoxygenated active site is in the high oxygen affinity state (R-state). In the Appendix, to validate the DFT results, we report also the energy profiles computed for model 1 using the CASSCF-CASPT2 approach.

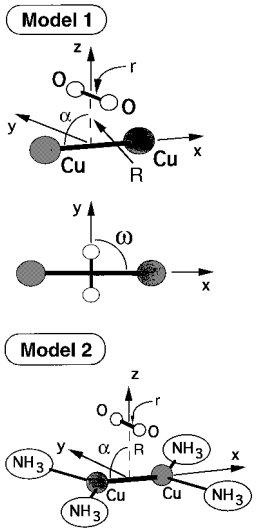

Figure 3. The two models used to emulate the oxygen binding site of hemocyanin and the symbols used for the relevant geometrical parameters. ω is the dihedral angle between the *yz* plane (which contains the dioxygen) and the *xz* plane (which contains the copper dimer).

Computational Methods

The DFT computations in the Kohn−Sham formulation[8] have been carried out with the DGauss 2.3.1 program.[9] We have used the local spin density approximation (LSD) for the exchange-correlation potential in the form given by Vosko, Wilk, and Nusair.[10a] Furthermore, we have considered nonlocal spin density corrections (NLSD) based on the Becke−Perdew functional.[10b] An LSD-optimized basis set of double-ζ quality in the valence shell plus polarization functions (DZVP) has been used.[11]

(4) (a) Himmelwright, R. S.; Eickman, N. C.; LuBien, C. D.; Lerch, K.; Solomon, E. I. *J. Am. Chem. Soc.* **1980**, *102*, 7339. (b) Solomon, E. I.; Penfield, K. W.; Wilcox, D. E. *Struct. Bonding* **1983**, *53*, 1. (c) Solomon, E. I. *Pure Appl. Chem.* **1983**, *55*, 1069. Himmelwright, R. S.; Eickman, N. C.; Solomon, E. I. *J. Am. Chem. Soc.* **1979**, *101*, 1576.

(5) (a) Brown, J. M.; Powers, L.; Kincaid, B.; Larrabee, J. A.; Spiro, T. G. *J. Am. Chem. Soc.* **1980**, *102*, 4211. Woolery, G. L.; Powers, L.; Winkler, M.; Solomon, E. I.; Spiro, T. G. *J. Am. Chem. Soc.* **1984**, *106*, 86. (c) Woolery, G. L.; Powers, L.; Winkler, M.; Solomon, E. I.; Lerch, K.; Spiro, T. G. *Biochim. Biophys. Acta* **1984**, *788*, 155.

(6) (a) Ross, P. K.; Solomon, E. I. *J. Am. Chem. Soc.* **1991**, *113*, 3246. (b) Solomon, E. I.; Baldwin, M. J.; Lowery, M. D. *Chem. Rev.* **1992**, *92*, 521. (c) Solomon, E. I.; Lowery, M. D. *Science* **1993**, *259*, 1575. (d) Maddaluno, J.; Giessner-Prettre, C. *Inorg. Chem.* **1991**, *30*, 3439. (e) Eisenstein, O.; Giessner-Prettre, C.; Maddaluno, J.; Stussi, D.; Weber, J. *Arch. Biochem. Biophys.* **1992**, *296*, 247. (f) Bernardi, F.; Bottoni, A.; Casadio, R.; Fariselli, P.; Rigo, A. *Int. J. Quantum Chem.* **1996**, *58*, 109.

(7) Andersson, K.; Malmqvist, P.; Roos, B. O.; Sadlej, A. J.; Wolinski, K. *J. Phys. Chem.* **1990**, *94*, 5483. Andersson, K.; Malmqvist, P.; Roos, B. O. *J. Chem. Phys.* **1992**, *96*, 1218.

For both model 1 and model 2 an energy profile along the reaction coordinate *R* (i.e. the distance between the center of mass of the copper dimer and that of the oxygen molecule) has been obtained for the singlet and triplet states. The geometry has been optimized at each point using the gradient method available in the DGauss program. During the geometry optimization the Cu−Cu distance has been kept fixed at the experimental value of 3.54 Å. For model 2 we have also kept the Cu−N bond lengths fixed at the experimental distances found between Cu and the histidine molecules (see Figure 1) and we have optimized only the structure of the NH_3 molecules (i.e. the N−H bond length and the HNH angle) and their orientation with respect to the Cu(O−O)Cu frame (rotation around the Cu−N axis).

Results and Discussion

The DFT energy values obtained for model 1 and model 2, together with the optimum geometrical parameters and the net atomic charges, are reported in Table 1. The corresponding energy profiles are represented in Figure 4. From this figure it is evident that for model 1 the triplet state is the ground state for all values of *R* (at $R = 0.0$ Å the energy gap is 3.9 kcal/mol). A minimum has been located on both the singlet and triplet curves, and the optimum structure of these two minima corresponds to a side-on configuration. In the singlet state the two oxygen atoms are in the same plane of the copper dimer ($R = 0.0$ Å) while in the triplet state *R* is 0.5 Å. The O−O bond length in the singlet complex is 1.41 Å, which is identical with the experimental value. However, at this level of theory the indication for a formal oxidation to cupric copper due to the oxygen bonding is not evident, the net charges on copper and oxygen in the singlet state being +1.28 and −0.28, respectively. These results indicate that model 1 is inadequate to emulate the oxygen binding process, since the approach of the oxygen molecule to the copper dimer leads to the formation of a triplet ground state complex, in contrast with the experimental evidence.

The problem has been reinvestigated using the same computational approach on the more complex model, which includes four in-plane NH_3 molecules (model 2). These new results show that the ligands play a fundamental role in determining the shape of the singlet and triplet potential surfaces and their relative energies. From Figure 4b we can see that at long distances the triplet is lower in energy than the singlet; furthermore, the triplet energy decreases until $R = 0.75$ Å and then increases and becomes rapidly higher than the singlet. Consequently, the ground state of the system is a triplet at the asymptotic limit (noninteracting triplet O_2 + hemocyanin) but becomes a singlet at bond distances via an intersystem crossing which occurs at about 0.75 Å. For values of *R* smaller than 0.75 Å, the singlet−triplet energy gap increases and becomes greatest at $R = 0.0$ Å (28.3 kcal/mol). Thus, the binding process requires the approaching of the oxygen molecule to the hemocyanin active site along the attractive triplet curve to reach the intersystem crossing point; after the crossing the process follows the singlet curve, leading to the formation of the final singlet complex (oxygenated protein).

Table 1. Relative Energies (*E*),[a] Optimum Values of the r_{O-O} Bond,[b] and Mulliken Net Charges (*q*) Computed for Model 1 and Model 2 in the Singlet (S_0) and Triplet (T_1) States at the DFT Computational Level for Various Values of the Approaching Distance *R*[b,c]

R	*E*[d]	r_{O-O}	$q(Cu_1)$	$q(Cu_2)$	$q(O_1)$	$q(O_2)$
			Model 1			
			S_0 State			
0.00	8.6	1.41	1.28	1.28	−0.28	−0.28
0.50	11.1	1.39	1.22	1.22	−0.22	−0.22
1.00	22.0	1.37	1.12	1.12	−0.12	−0.12
1.50	39.4	1.31	1.04	1.04	−0.04	−0.04
2.00	56.9	1.27	0.98	0.98	0.02	0.02
10.0	70.6	1.24	1.00	1.00	0.00	0.00
			T_1 State			
0.00	4.7	1.39	1.21	1.21	−0.21	−0.21
0.50	0.0	1.37	1.17	1.17	−0.17	−0.17
1.00	1.1	1.34	1.08	1.08	−0.08	−0.08
1.50	14.1	1.30	1.00	1.00	0.00	0.00
2.00	23.3	1.26	0.94	0.94	0.06	0.06
10.0	33.4	1.24	1.00	1.00	0.00	0.00
			Model 2			
			S_0 State			
0.00	0.0	1.47	0.76	0.78	−0.46	−0.41
0.50	5.8	1.44	0.69	0.71	−0.39	−0.28
0.75	12.9	1.42	0.64	0.66	−0.31	−0.25
1.00	23.3	1.40	0.59	0.61	−0.26	−0.25
1.50	49.9	1.34	0.54	0.56	−0.18	−0.17
2.00	69.0	1.30	0.49	0.50	−0.11	−0.10
3.00	86.1	1.25	0.43	0.45	−0.03	−0.02
10.0	88.4	1.24	0.43	0.44	0.00	0.00
			T_1 State			
0.00	28.3	1.46	0.76	0.78	−0.43	−0.38
0.50	14.1	1.42	0.69	0.71	−0.39	−0.28
0.75	11.8	1.40	0.64	0.66	−0.31	−0.25
1.00	14.3	1.38	0.59	0.60	−0.23	−0.20
1.50	30.3	1.32	0.51	0.52	−0.14	−0.12
2.00	43.7	1.28	0.45	0.46	−0.05	−0.03
3.00	50.2	1.25	0.42	0.43	0.01	0.02
10.0	51.3	1.24	0.43	0.44	0.00	0.00

[a] Values in kcal/mol. [b] Bond lengths in angstroms. [c] The optimum value for the ω and α angles is 90° for all values of *R*. [d] Total energy value for the triplet complex ($R = 0.5$ Å) of model 1: −3430.554 33 au. Total energy value for the singlet complex ($R = 0.0$ Å) of model 2: −3657.247 50 au.

The geometry of the ground-state singlet complex remains similar to that found for model 1 at the same level of theory. The copper and oxygen atoms lie again in the same plane in a side-on configuration, but the O−O distance becomes longer than in the absence of ligands, i.e. 1.47 Å, a value which is still in rather good agreement with that found in the crystal of the oxygenated *Limulus* hemocyanin (1.41 Å). At the triplet minimum the dioxygen is still in a side-on configuration and the distance *R* is 1.46 Å. Another important result concerns the singlet electron distribution, which shows that, in the presence of ligands, the charge transfer from the copper atoms to dioxygen becomes much more significant, in agreement with the experimental evidence: the net atomic oxygen charges are in fact −0.46 and −0.41 (the lack of symmetry in the atomic charges is due to the different values of the experimental Cu−N distances used in the computations). However, since a simultaneous charge transfer occurs from the ammonia molecules to the copper atoms, the final net metal charges are +0.76 and +0.78. The values reported in Table 1 show that the charge transfer from coppers to oxygens decreases rapidly with the increase of the distance *R* and becomes negligible at $R = 3.0$ Å.

The effect of ligands on the energy order of the singlet and triplet states can be rationalized using a simple orbital interaction

(8) Hohenberg, P.; Kohn, W. *Phys. Rev. B* **1964**, *136*, 864. Kohn, W.; Sham, L. J. *Phys. Rev. A* **1965**, *140*, 1133.
(9) UniChem DGauss, Version 2.3.1, Cray Research, Inc., **1994**. This version, where the authors have implemented the computation of the Hessian matrix used in the geometry optimization, provides geometries which are slightly different but more accurate than those obtained with the previous version 2.1 and used in ref 6f.
(10) (a) Vosko, H.; Wilk, L.; Nusair, M. *Can. J. Phys.* **1980**, *58*, 1220. (b) Becke, A. D. *Phys. Rev. A* **1988**, *38*, 3098. Perdew, J. P. *Phys. Rev. B* **1986**, *33*, 8822. (c) Becke, A. D. *J. Chem. Phys.* **1993**, *98*, 1372. (d) Parr, R. G.; Yang, W. *Density-Functional Theory of Atoms and Molecules*; Oxford University Press: New York, 1989.
(11) Godbout, N.; Salahub, D. R.; Andzelm, J.; Wimmer, E. *Can. J. Chem.* **1992**, *70*, 560.

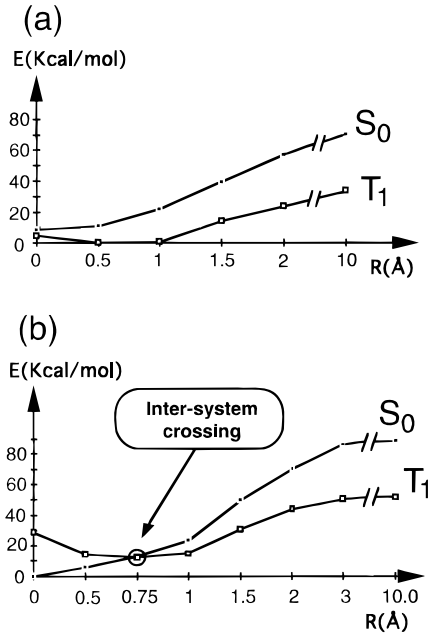

Figure 4. Potential energy curves computed for (a) model 1 and (b) model 2 for the singlet state S_0 and the triplet state T_1 at the DFT computational level.

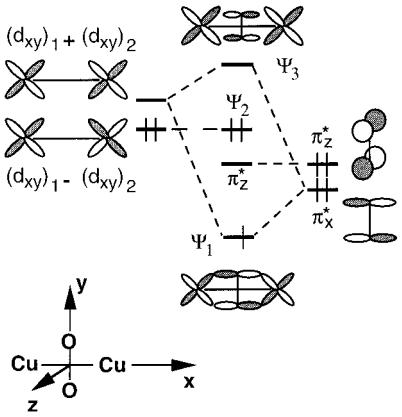

Figure 5. Correlation diagram which describes the orbitals involved in the bonding between the copper dimer and the oxygen molecule in the S_0 state.

model (the orbital interactions for similar systems involving a copper dimer have been already discussed by Sherwood and Hoffmann[12]). In this model we must consider first the orbitals which are involved in the bonding between the oxygen molecule and the copper ion dimer, i.e. the two copper orbitals $(d_{xy})_1$ and $(d_{xy})_2$ and the π_x^* and π_z^* dioxygen orbitals. These orbitals and their interactions, occurring when the O_2 molecule approaches the protein active site, are illustrated in Figure 5. The two d_{xy} orbitals of the copper dimer form an in-phase $(d_{xy})_1 - (d_{xy})_2$ and an out-of-phase $(d_{xy})_1 + (d_{xy})_2$ linear combination. These two combinations are very near in energy, since the two copper ions are far away (3.54 Å) and the overlap is small. When the dioxygen approaches the copper dimer, the interaction between the $(d_{xy})_1 + (d_{xy})_2$ out-of-phase combination and the π_x^* orbital leads to the formation of the lower energy orbital ψ_1 and the higher energy orbital ψ_3. The in-phase combination $((d_{xy})_1 - (d_{xy})_2 \Leftrightarrow \psi_2)$ and the π_z^* oxygen orbital cannot interact by symmetry and remain almost unchanged. The orbital occupancy (π_x^* and π_z^* orbitals doubly occupied, in-phase combination $(d_{xy})_1 - (d_{xy})_2$ doubly occupied, and out-of-phase combination $(d_{xy})_1 + (d_{xy})_2$ empty) is that of the final complex

(12) Sherwood, P.; Hoffmann, R. *Inorg. Chem.* **1989**, *28*, 509.

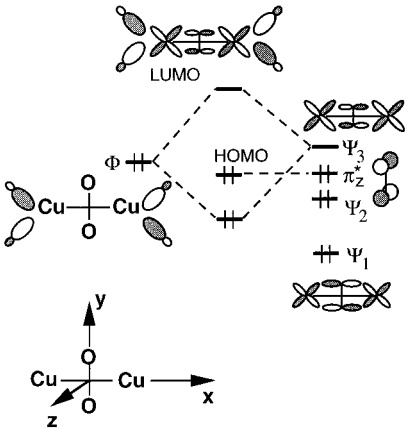

Figure 6. Correlation diagram which describes the interaction between the ligand lone pairs and the LUMO (Ψ_3) of the $Cu^{2+}(O-O)^{2-}Cu^{2+}$ system.

and is determined by the electron transfer (experimentally observed) occurring, upon oxygen binding, from the Cu^+ cations of the deoxygenated protein to dioxygen. This occupation pattern represents the dominant configuration in the CASSCF singlet (S_0) wave function.[6f] The two lowest T_1 and T_2 triplet states can be obtained from S_0 by moving one electron from π_z^* to Ψ_3 (T_1) or from Ψ_2 to Ψ_3 (T_2). Thus, in the T_1 configuration the π_z^* and Ψ_3 orbitals are singly occupied, while in the T_2 configuration the two unpaired electrons are in the two orbitals Ψ_2 and Ψ_3. The diagram of Figure 5 indicates that the interaction between the $(d_{xy})_1 + (d_{xy})_2$ orbital and the π_x^* dioxygen orbital determines the HOMO−LUMO energy gap. It has already been suggested[13] that we can focus on this energy difference as a measure of the singlet−triplet energy splitting: if the HOMO and LUMO are very close in energy, the triplet state is lower in energy than the singlet state and represents the ground state of the system, while a significant splitting between the two orbitals will cause the singlet to be the ground state. In the present case, when we consider model 1, the interaction between $(d_{xy})_1 + (d_{xy})_2$ and π_x^* and the relative splitting are not large enough and the triplet T_1 is the ground state.

We consider now the additional orbital interactions which occur when the ligands are added to the model (model 2). These interactions are illustrated in Figure 6 and involve the four nitrogen lone pairs and the orbitals of the $Cu^+(O-O)Cu^+$ fragment (the energy order of these orbitals is that found at the DFT level). The high-energy out-of-phase combination of the four nitrogen lone pairs (Φ) has the right symmetry to interact with the Ψ_3 orbital. This interaction leads to a lower energy combination which is doubly occupied and to a higher energy combination which is empty and which becomes the LUMO. For symmetry reasons the HOMO (which is almost completely dominated by the dioxygen π_z^* orbital) cannot interact with the nitrogen lone pairs and, consequently, its energy is not significantly affected by the presence of ligands. The final effect is that the introduction of ligands increases the HOMO−LUMO energy gap which, at bond distances, becomes large enough to make the singlet state lower in energy than the triplet state. The addition of two axial ligands does not significantly change the HOMO−LUMO energy gap, since they are far away from the copper dimer (the Cu−N distances are 2.77 and 2.66 Å) and the overlap is small. This explains why the singlet−triplet energy gap does not change very much when we include in the

(13) (a) Salem, L.; Rowland, C. *Angew. Chem., Int. Ed. Engl.* **1972**, *11*, 92. (b) Hay, P. J.; Thibeault, J. C.; Hoffmann, R. *J. Am. Chem. Soc.* **1975**, *97*, 4884.

model two additional NH_3 molecules, as demonstrated in ref 6f, and indicates that model 2 is adequate.

Conclusions

In this paper we have investigated the mechanism of the oxygen binding process to hemocyanins using a DFT approach on two different model systems. The simpler model (model 1) is formed only by the Cu^+-Cu^+ dimer and the approaching oxygen molecule, while the more complex model (model 2) also includes four NH_3 molecules, which emulate the real in-plane histidine ligands.

The results obtained for model 1 have pointed out the inadequacy of a simple model, with no ligands to the copper atoms, to describe properly the binding process of the oxygen to the hemocyanin active site. In the absence of ligands, in fact, the results indicate that the triplet state T_1 remains the ground state along the whole reaction path, in contrast with the experimental evidence, which shows that the final oxyhemocyanin complex is a singlet.

The process has also been studied on a more reliable model which includes the copper ligands. These computations have demonstrated that the ligands are responsible for the greater stability of the singlet versus the triplet state at bonding distance and for the occurrence of an intersystem crossing along the reaction coordinate *R*. In the process of binding, the oxygen approaches the hemocyanin active site, moving along the triplet curve to reach the crossing point at $R = 0.75$ Å, and then proceeds along the attractive singlet curve to form the final singlet complex experimentally observed.

This finding shows that the greater stability of the singlet versus the triplet state is not an intrinsic property of the oxygenated form of the copper dimer but depends on the presence of the ligands to the copper atoms. The ligand effect has been rationalized on the basis of a simple orbital interaction model and the assumption that we can focus on the HOMO−LUMO energy difference as a measure of the singlet−triplet energy splitting. The key orbital interaction outlined by this model is that occurring between the out-of-phase combination of the nitrogen lone pairs and the LUMO of the $Cu^+(O-O)-Cu^+$ system. When the approaching distance *R* decreases, this interaction becomes responsible for the increase of the HOMO−LUMO energy gap, which makes the singlet state more stable than the triplet state and determines the appearance of an intersystem crossing.

Acknowledgment. R.C. acknowledges a grant for computational time at CINECA.

Appendix: CASSCF and CASPT2 Computations for Model 1

To validate the DFT analysis, we have computed for model 1 the energy profiles along the reaction coordinate *R* for the singlet state S_0 and the two lowest triplet states T_1 and T_2 at the CASSCF and CASPT2 levels of theory. The energy values are reported in Table 2, and the resulting energy profiles are represented in Figure 7. All the CASSCF and CASPT2 computations have been carried out with MOLCAS-2 software[14] using the MIDI4 basis set of Tatewaki and Huzinaga.[15] At the CASSCF level the geometry has been optimized with the gradient method under the constraint of a fixed Cu−Cu distance (Cu−Cu = 3.54 Å). At the CASPT2 level we have optimized only the O−O bond length (*r*) with the α and *ω* angles kept fixed at 90°. In this case the optimization has been performed by fitting the computed energies for different values of *r* to a second-degree polynomial. The active space includes, in addition to the orbitals illustrated in Figure 4, also the *σ* and *σ** orbitals associated with the O−O bond.

Table 2. Relative Energies (*E*),[a] Optimum Values of the r_{O-O} Bond,[b] and Mulliken Net Charges (*q*) Computed for Model 1 in the Singlet (S_0) and Triplet (T_1, T_2) States at the CASSCF and CASPT2 Computational Levels for Various Values of the Approaching Distance *R*[b,c]

R	*E*[d]	r_{O-O}	*q*(Cu)	*q*(O)
		CASSCF		
		S_0 State		
0.00	0.0	1.76	1.64	−0.64
0.50	14.2	1.74	1.62	−0.62
1.00	41.1	1.40	0.99	0.01
2.00	30.0	1.34	0.97	0.03
3.00	33.3	1.32	0.99	0.01
10.00	35.5	1.31	1.00	0.00
		T_1 State		
0.00	49.3	1.48	1.13	−0.13
0.50	40.8	1.42	1.07	−0.07
1.00	25.2	1.35	1.00	0.00
2.00	10.7	1.31	0.97	0.03
3.00	14.5	1.31	0.99	0.01
10.00	16.5	1.29	1.00	0.00
		T_2 State		
0.00	3.5	1.79	1.65	−0.65
0.50	16.2	1.75	1.62	−0.62
		CASPT2		
		S_0 State		
0.00	44.4	1.58	1.64	−0.64
0.50	55.1	1.51	1.62	−0.62
1.00	43.1	1.44	0.98	0.02
2.00	40.1	1.35	0.96	0.04
3.00	51.0	1.34	0.98	0.02
10.00	51.9	1.33	1.00	0.00
		T_1 State		
0.00	0.0	1.50	1.26	−0.26
0.50	19.7	1.48	1.31	−0.31
1.00	13.4	1.39	1.00	0.00
2.00	15.7	1.33	0.97	0.03
3.00	23.8	1.30	0.98	0.02
10.00	27.9	1.30	1.00	0.00
		T_2 State		
0.00	61.6	1.72	1.65	−0.65
0.50	67.3	1.66	1.63	−0.63

[a] Values in kcal/mol. [b] Bond lengths in angstroms and angles in degrees. [c] The optimum value of the *ω* and α angles is 90° for all values of *R*. [d] Total energy value for the singlet complex ($R = 0.0$ Å) computed at the CASSCF level: −3423.313 00 au. Total energy value for the triplet complex ($R = 0.0$ Å) computed at the CASPT2 level: −3434.222 00 au.

At the CASSCF level both the singlet (S_0) and the triplet (T_2) curves show a minimum at $R = 0.0$ Å, with the singlet minimum lower in energy than the triplet minimum (3.5 kcal/mol); thus, in the absence of dynamic correlation contributions, the ground state at bond distances is a singlet, as we have already pointed out.[6f] The triplet state T_1 is unbound at $R = 0$ Å but shows a shallow minimum at about 2.0 Å. This state correlates with the electronic situation of the isolated triplet O_2 and, at the asymptotic limit, becomes the ground state. When *R* is large enough (values greater than 1.0 Å), the S_0 state becomes about 16−19 kcal/mol higher in energy than T_1; the T_2 state is much more destabilized, and its energy is too high to be included in the diagram. The two curves S_0 and T_1 cross at about 0.8 Å, and thus the change from the most stable situation at the asymptotic limit (triplet T_1) to the most stable situation at

(14) MOLCAS version 2: Andersson, K.; Fulscher, M. P.; Lindth, R.; Malmqvist, P.; Olsen, J.; Roos, B. O.; Sadlej, A. J.; Widmark, P. O. University of Lund, Sweden, and IBM Sweden, 1991.
(15) Tatewaky, H.; Huzinaga, S. *J. Comput. Chem.* **1980**, *1*, 205.

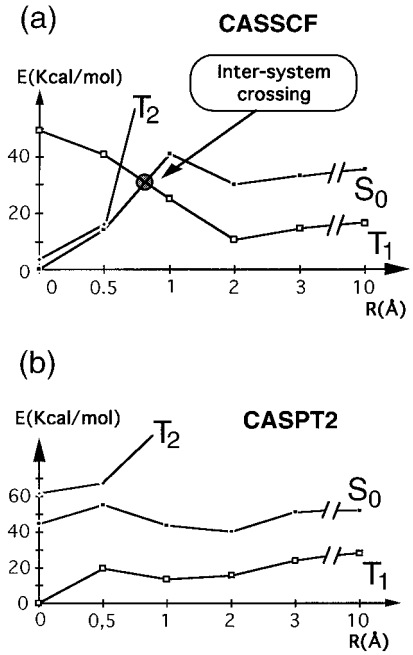

Figure 7. Potential energy curves computed for model 1 for the singlet state S_0 and the triplet states T_1 and T_2 at the CASSCF (a) and CASPT2 (b) computational levels.

bonding distance (singlet S_0) occurs via an intersystem crossing. The barrier which must be overcome to reach the point of intersection is about 15 kcal/mol.

The energetics obtained at the CASSCF level are not expected to be reliable, since most of the dynamic correlation energy is neglected. The CASPT2 results illustrate this point. We can see that at this level of theory (Figure 7b) the ground state of the system is the triplet T_1 for all values of R so that the intersystem crossing point disappears. The triplet T_2 remains always higher than S_0 (17.2 kcal/mol at $R = 0.0$ Å) and its energy increases rapidly with the increase of the reaction coordinate R. The inclusion of dynamic correlation energy also affects the geometry: the optimum O−O bond distance in the singlet complex ($R = 0.0$ Å) becomes 1.58 Å, which is in better agreement with the experimental value than the CASSCF value (1.76 Å). All these results are in qualitative agreement with the DFT computations (even if the DFT singlet−triplet energy gap is much larger) and confirm the importance of the dynamic correlation to obtain a reliable description of both the geometry and energetics of these systems.

The effect of the dynamic correlation which inverts the energy order of the electronic states can be understood from the interaction diagram of Figure 4. The inclusion of correlation (CASPT2 and DFT computations) lowers the energies of the whole set of orbitals which describe the bonding between the copper dimer and the oxygen molecule.[16] However, this orbital energy lowering must be more significant for the Ψ_2 and Ψ_3 orbitals than for the π_z^* orbital since Ψ_2 and Ψ_3 correspond to a much more crowded electronic arrangement (the d_{xy} copper orbital contributions are in fact dominant).[18] The final effect is that the inclusion of the dynamic correlation makes the orbital Ψ_2 lower in energy than π_z^*, which becomes the HOMO, as found in the DFT computations. As a consequence of this differential energy lowering, the HOMO−LUMO energy splitting decreases and the triplet T_1 (where the π_z^* orbital is singly occupied) becomes the ground state.

IC960102J

(16) This effect has been verified on model 1 by means of DFT computations performed with the Gaussian 92 program[17] at two different levels of approximation: in one case we have considered only the exchange functional suggested by Becke,[10c] while in the other case we have also included the correlation functional proposed by Lee, Yang and Parr.[10d]

(17) Gaussian 92/DFT, Revision G.1: Frisch, M. J.; Trucks, G. W.; Schlegel, H. B.; Gill, P. M. W.; Johnson, B. G.; Wong, M. W.; Foresman, J. B.; Robb, M. A.; Head-Gordon, M.; Replogle, E. S.; Gomperts, R.; Andres, J. L.; Raghavachari, K.; Binkley, J. S.; Gonzalez, C.; Martin, R. L.; Fox, D. J.; Defrees, D. J.; Baker, J.; Stewart, J. J. P.; Pople, J. A. Gaussian, Inc., Pittsburgh PA, 1993.

(18) Bernardi, F.; Bottoni, A.; Celani, P.; Olivucci, M.; Robb, M. A.; Venturini, A. *Chem. Phys. Lett.* **1992**, *192*, 229.